ACADEMIA ROMÂNĂ
Revue Roumaine de Chimie
http://web.icf.ro/rrch/

Rev. Roum. Chim.,
2012, *57*(4-5), 435-442

Dedicated to Professor Ionel Haiduc
on the occasion of his 75th anniversary

THEORETICAL STUDY OF THE REACTION OF $LiBH_4$ WITH MgH_2 IN PRESENCE OF CARBON SUBSTRATE

Viorel CHIHAIA,[a,b,*] Cornel MUNTEANU,[a] Rares SCURTU[a] and Petru PALADE[c]

[a] "Ilie Murgulescu" Institute of Physical Chemistry of the Romanian Academy, 202 Splaiul Independentei, Sector 6, 060021 Bucharest, Roumania; e-mails: vchihaia@icf.ro, munteanuc@icf.ro, rscurtu@icf.ro
[b] Division Computational Science, Jülich Supercomputing Centre, Wilhelm-Johnen-Straße, 52425 Jülich, Germany; e-mail: v.chihaia@fz-juelich.de
[c] National Institute of Materials Physics, 105 bis Atomistilor str., PO Box MG. 7, 077125 Magurele, Bucharest, Romania; e-mail: palade@infim.ro

Received December 13, 2010

In this work we design some atomic scale simulation methods as investigative tools in the study of the formation of compounds for the reversible storage of hydrogen in bulk materials. It was verified that the reaction between the $LiBH_4$ and MgH_2 is energetically favored for temperatures above 280 K and that this system can be used in the hydrogen storage and the fuel cell application. To identify the reaction mechanism at the interface of $LiBH_4$, MgH_2 and carbon layers we performed some Molecular Dynamics simulations and QM/MM calculations. The results show that the layers of ions formed at the interface with the graphite may assure the right arrangement of the atoms to start the formation of the crystals. Moreover, the presence of the hexagonal layers of graphite may play a role as a pattern template for the layers of boron atoms in the MgB_2 lattice.

INTRODUCTION

Hydrogen is considered after its combustion the most ecological fuel, the resulting product being the pure water. Therefore, it could be the future fuel. Fundamental research studies are necessary for the optimization of the costs related to the materials and the energy consumed. The current methods used for the hydrogen storage are the molecular hydrogen compression in high pressure vessels and the storage at low temperatures in liquid form and as chemical compounds, such as the metal hydrides. The liquid hydrogen storage technology is well established, but the energy cost of liquefaction is still high and some technological improvements are necessary. Storing hydrogen in metal hydride is a safe method, but problems related to the amount of hydrogen stored in the total weight of the compound are still unsolved. The hydrogen storage within systems that show pores (glass, silicates), channels (nanotubes, zeolites), cavities (zeolites, clathrate) or high specific surfaces (nanofibres) could be alternative methods.

Magnesium is one of the most attractive material for the hydrogen storage with a capacity of up to 7.6% of the total mass (wt%). Since the reaction rate of hydrogen adsorption / desorption is very low, the elemental magnesium is not of practical importance. Magnesium compounds show a higher reaction speed. $LiBH_4$ is of great interest because it may contain hydrogen up to 18.5 wt%.[1] There are still problems because of the low reaction kinetics and the high thermodynamic stability of $LiBH_4$. The reverse reaction occurs at a

* Corresponding author: vchihaia@icf.ro

high temperature, 500°C. The enthalpy of the decomposition reaction can be reduced in the reaction with MgH_2

$$2\cdot LiBH_4(s) + MgH_2(s) \longleftrightarrow 2\cdot LiH(s) + MgB_2(s) + 4H_2(g) \quad (1)$$

with a release of molecular hydrogen in quantities of up to 10.5 wt.%.[2] The reverse reaction is reduced due to the high stability of the MgB_2 component. Vajo found that the rate of reaction (1) is improved by mechanical milling, with resulting hydrogen in a quantity of more than 11 wt%. The kinetics can be improved in presence of additives.[3] Carbon-based additives, in particular grinding nanotubes, enhance the reaction thermodynamics.[4] The infiltration of $LiBH_4$ in nanoporous carbon leads to an improved desorption kinetics and reaction reversibility.[5]

In the present study we characterize the reaction (1) that can occur at the interfaces of $LiBH_4$ / MgH_2/graphite through quantum and thermodynamic calculations and through molecular dynamics simulations.

COMPUTATION METHODS

1. Thermodynamic Calculations

The reaction (1) is of type

$$\sum_i r_i R_i \longleftrightarrow \sum_j p_j P_j + nH_2(g)$$

where the reactants R_i and the reaction products P_j are considered in the crystalline state and the molecular hydrogen in the gas phase. The Gibbs free energy variation for this reaction is written as

$$\Delta G_{reaction} = \Delta G_{products} - \Delta G_{reactants}$$

where $G_{reactants} = \sum_i r_i G_i$ and $G_{products} = \sum_j p_j G_j + nG_{H_2}$ are the summations of the Gibbs free energy of each substance.

The free energy of the crystal systems is given by $G \cong U(0) + U_{vib}(T) - TS_{vib}(T) + PV$, where $U(0)$ is the internal energy of the crystal, which includes the zero point energy (ZPE), $U_{vib}(T)$ is the vibration term, $S_{vib}(T)$ is the system entropy, T and V are the system temperature and volume, and P is the pressure.[6]

Because the volume associated to the hydrogen molecular gas is large in comparison with that of the crystals, the contribution of the term PV to the crystalline components can be neglected, $\Delta(PV)_{cris} \cong 0$. Moreover, we neglect the change of the crystal volume with the temperature $V \neq V(T)$. It changes with the pressure applied to the system $V = V(P)$. The anharmonic component of the vibration contribution to the total internal energy $U_{vib}(T)$ and the entropy $S_{vib}(T)$ can be neglected for low temperatures.

If the vibration density of state is known, then the harmonic contribution to the internal energy can be computed as

$$U_{harmon}(V,T) = \int_0^\infty g(\omega,T)\frac{h\omega}{2th(\beta h\omega/2)}d\omega$$

where $\beta = 1/kT$, k is the Boltzmann constant, and $g(\omega,T)$ is the phonon density of states and ω is the angular frequency. The zero point energy contribution is given by $U_{ZPE} = \frac{1}{2}\int g(\omega)h\omega\, d\omega$.

The contribution of the vibration to the entropy is

$$S_{vib}(T) = k\left[\int_0^\infty g(\omega,T)\frac{\beta h\omega}{e^{\beta h\omega}-1}d\omega - \int_0^\infty g(\omega,T)\left(1-e^{-\beta h\omega}\right)d\omega\right]$$

The molecular hydrogen gas behaves like an ideal one, for which we may write[7]

$$G_{H_2} = U_{H_2}(0) + U_{transl+rot}(T) + U_{vib,H_2} + (PV)_{H_2}$$

where $U_{H_2}(0)$ is the total energy plus the zero vibration energy of the hydrogen molecule. The other components can be written as $U_{transl+rot}(T) = \frac{5}{2}RT$, the translation and rotation energy of the hydrogen molecule, $U_{vib,H_2} = \frac{N_A h\omega}{2} + \frac{N_A h\omega e^{-\beta h\omega}}{1-e^{-\beta h\omega}}$, the component of the total energy given by the vibration of the hydrogen molecule. The vibration frequency ω of the hydrogen molecule can be determined with high accuracy in ab-nitio or DFT calculations.

Finally, the Gibbs free energy change can be written as $\Delta G_{reaction} = \Delta G_{cris} + G_{H_2}$, where ΔG_{cris} is the change of the Gibbs free energy corresponding to the crystalline phase.

To calculate the free energy variation corresponding to reaction (1) we have performed DFT calculations with the solid-state software

ABINIT[8] to determine the equilibrium geometry of each crystal or molecular system, the corresponding internal energy (electronic and ZPE) and the phonon density of states. The exchange and correlation potentials are of the type PW91.[9] The cut-off limit of the plane-wave basis is 700.0 eV. To balance the computing speed and the memory required, the full geometry optimization (fractional coordinates of atoms and elementary cell parameters) was done by using the BFGS algorithm. The convergence tolerance limit for the total energy of 10^{-5} eV was chosen, which is equivalent to a maximum tolerance limit of 5.10^{-2} GPa for the stress tensor components.

Phonon frequencies and the density of states can be calculated from the derivative of the energy (phonon freeze method)[10] or from the forces of each atom in the frame of the Hellman-Feyman theorem (linear response method).[11] The phonon freeze method requires a large supercell to avoid the interactions of the atoms with their images. Therefore, in order to reduce the computational effort we use linear response method.

2. Molecular Dynamics

To obtain information about the reaction pathway we did some reactive molecular dynamics studies for the interface $LiBH_4$ / MgH_2 / graphite. The system is represented in Figure 2 and is obtained by assembling a supercell 4x2x6 for MgH_2, a supercell 2x2x4 for $LiBH_4$ and 4 layers of graphite. The rhombic unit cell of graphite is changed into a tetragonal one through the transformation $\begin{pmatrix} 1 & 1 & 0 \\ -1 & 1 & 0 \\ 0 & 0 & 1 \end{pmatrix}$. To create these interfaces, the surfaces (001) of the supercells were chosen in the plane of the interfaces. A 3D periodicity is applied to the system obtained. The cell constants in the interface plane are an average of the corresponding parameters of the individual cells.

Molecular dynamics calculations were performed at the temperature T = 300K by using the atomic scale simulation package Gulp.[12] This code allows the fitting of a large number of empirical force fields, the optimization of the 0D-3D atomic structures in conditions in which some atoms can be completely frozen or only along certain directions. The code is able to perform Molecular Dynamics and Monte Carlo simulations.

The time evolution of the atomic positions and the velocities were assessed within the Verlet integration scheme with a time step of 0.5 fs. To relax the tension induced in the final system, the system is fully optimized (supercell constants and fractional coordinates of atoms) under the constraints of the tetrahedral box. The cell thus obtained is further pre-equilibrated in a short NVT Molecular Dynamics simulation (50 ps) until the total energy is stabilized. The temperature is kept fixed at a value of 300 K by velocity scaling. The simulation is continued for other 4 ns, where the temperature is controlled by a Nosé thermostat with a time constant of 1 ps. To avoid complications caused by interference of the pressure reservoir with the system dynamics we chose to perform the simulations in a macrocanonical ensemble (NVT) and not in an isothermal-isobaric one (NPT), which corresponds to the experimental conditions. The equilibration was followed by additional 1 ns simulation in NVE ensemble, when the data are collected for the statistical analysis. The atom trajectories were saved every 5 fs for the statistical analysis.

Since we could not find in literature an empirical force field developed for the studied systems, we have investigated the accuracy of some force fields available in the program Gulp for such systems. We decided to use the empirical force field UFF (Universal Force Field)[13] which is parameterized for all chemical elements. Since this force field underestimates the lattice constants of the four crystals of interest, we reparameterized the UFF potential to reproduce the equilibrium geometries of the four crystals and the corresponding total energies.[14]

3. QM/MM Calculations

To characterize the reactivity at the interface of MgH_2 with $LiBH_4$ completely, we must also take into account the electronic structure. Preliminary calculations performed within the semiempirical method PM6[15] with parameterization included in the program MOPAC09,[16] in which we fully treated the interface $LiBH_4$ / MgH_2 (168 atoms = H_{112}, B_{16}, Li_{16}, Mg_{24}) at quantum level, show that at this interface some chemical reactions take place. Some of the reaction products are hydrogen molecules and groups of LiH. Because the quality of the method PM6 is questionable, we tested the hypothetical reactions by more precise calculation methods. The large number of atoms in the system interface $LiBH_4$ / MgH_2 limits the complete

quantum treatment. Therefore, we simulated the system by using the ONIOM method[17] of type QM / MM included in the program GAUSSIAN03.[18] Although the program GAUSSIAN03 is designed for quantum chemistry, it is able to treat 3D periodic systems by considering only the point Γ in the inverse space. The ONIOM method allows the study of large systems, by defining two or more domains of the system, which are treated at different level of accuracy. We used the same structure as in the molecular dynamics simulations. The atoms are treated with the empirical force field UFF, but the area of the interface $LiBH_4$ / MgH_2 (delimited by dashed lines in Fig. 5) is treated by quantum computing scheme PW91/6-31G* in Density Functional Theory. The system is relaxed by the optimization of the fractional coordinates of all atoms and of the lattice constant along the direction perpendicular to the interface.

RESULTS AND DISCUSSION

Thermodynamic analysis of the $LiBH_4 + MgH_2$ reaction

The parameters of the optimized crystalline systems, the interatomic distance of hydrogen molecule and the total internal energies corresponding to these systems are presented in Table 1.

Considering the energies corresponding to the equilibrium, we determine the reaction energy at T = 0K as 3.1862 eV (73.4 kcal/mol) and 2.2032 eV (50.8 kcal/mol), respectively, when ZPE correction is considered.

It can be seen that at T = 0 K the reaction energy is not favoured in the direct sense of the reaction (1), but the inverse reaction takes place freely.

Table 1

The equilibrium geometry parameters and the corresponding total energies for the crystalline systems and for the hydrogen molecule. Excepting the γ angle for MgB_2, which is 120°, all the other angles are 90°. The values in parentheses correspond to the experimental data

	Symmetry group	Unit cell parameters [Å]			Total Energy
		A	B	C	
$LiBH_4$	62 Pnma	7.1785 (7.1785)	4.4368 (4.4366)	6.8031 (6.8032)	-601.59290
MgH_2	136 P42/mnm	4.5287 (4.5168)	4.5287 (4.5168)	2.9952 (3.0205)	-112.93607
LiH	225 Fm-3m	3.9459 (4.0834)	3.9459 (4.0834)	3.9459 (4.0834)	-95.78858
MgB_2 $\gamma=120^o$	191 P6/mmm	3.0578 (3.0851)	3.0578 (3.0851)	3.5501 (3.5201)	-179.95103
H_2	$D_{h\infty}$	d_{HH} = 0.746			-31.55824

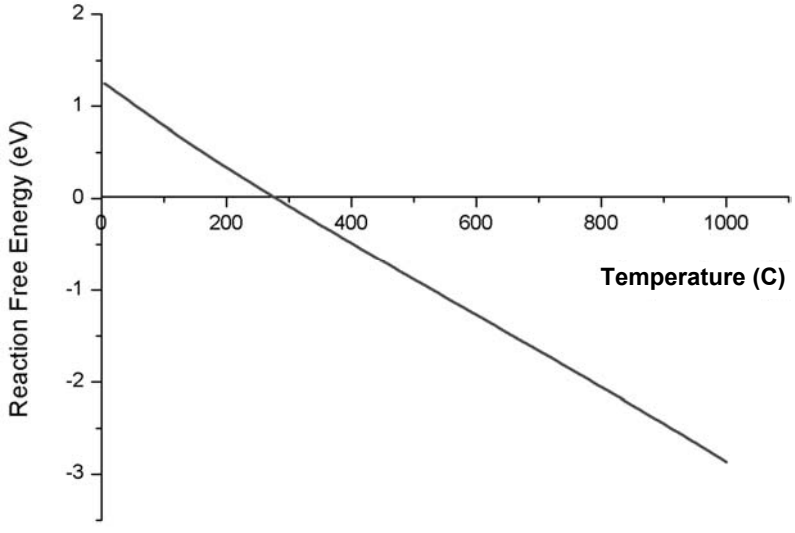

Fig. 1 – The dependence of the Gibbs free energy variation on temperature for reaction (1).

To see what the effect of temperature on reaction is, we calculate the Gibbs free energy of the crystalline systems and of the hydrogen molecule. We proved that all the frequencies in the phonon spectra have positive values, which shows that all the crystalline systems are in a stable equilibrium.

The temperature dependency of the variation of the Gibbs free energy for reaction (1) is presented in Fig. 1. We observe that the variation of the Gibbs free energy $\Delta G_{reaction} < 0$ is negative for temperatures above 280 °C, which is the temperature when the reaction (1) becomes exothermal. This temperature coincides with the one for which the $LiBH_4$ melts.[19] We must specify that the Gibbs free energies for crystal systems were calculated at P = 0 atm. These investigations can be extended by considering different volumes of the crystalline systems and calculating the density of the phonon states in these conditions. The pressure corresponding to the various states of contraction can be calculated based on the equations of state of Murnaghan type.[20]

Molecular Dynamics Studies for the $LiBH_4$ / MgH_2 / C interfaces

The thermodynamic calculations can be used to determine the reaction path by considering the intermediar reactions, but they do not clearly show the reaction mechanisms at the interface $LiBH_4$ / MgH_2. Therefore we did molecular dynamics simulations to investigate the mobility and the reactivity of the atoms within the interfaces $LiBH_4$ / MgH_2 / graphite. In the first 5 ps of molecular dynamics simulation the region that corresponds to the MgH_2 system is expanded and compresses the $LiBH_4$ and the graphite systems. After this stage, the diffusion of atoms begins. This dynamic is illustrated in Fig. 2.

By analyzing the time-averaged distributions of the atoms in the z direction perpendicular to the interface (see Fig. 3), it is found that the graphite layers remain intact.

The atoms of the $LiBH_4$ and MgH_2 structures diffuse through the interface $LiBH_4$ / MgH_2 and are arranged in layers at the interface with the graphite layers. Note the high peak of boron atoms at the interface with the graphite, which creates prerequisites for the formation of planar hexagonal network of boron, like in MgB_2, one of the products of the reaction (1). Thus, the layers of graphite can act as a patern maker for the boron layers. Note that the magnesium atoms diffuse to the other interface with the graphite. However, due to the high mobility of magnesium atoms, we can assume that they can penetrate between the patches of the boron layers, forming the crystal structure of MgB_2.

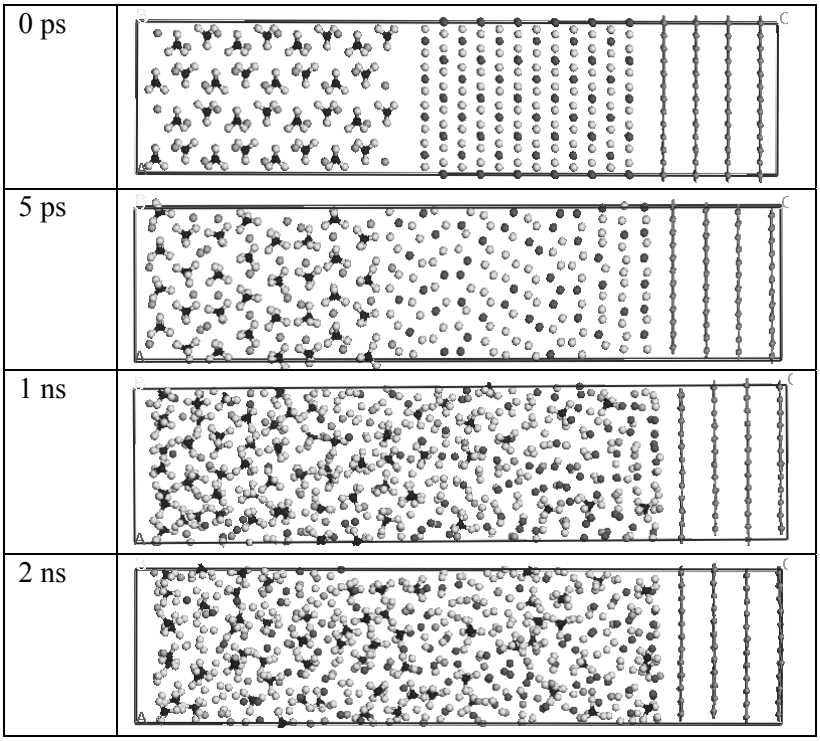

Fig. 2 – The system configurations at different time steps. The colour legend of the atoms: red - Magnesium, blue - Boron, yellow - Hydogen, pink - Lithium, gray - Carbon.

To investigate the formation of the products of reaction (1) we analyzed the radial distribution of various pairs of atoms. It can be seen that a specific peak for the pairs boron-hydrogen remains present in the crystal structure of $LiBH_4$, indicating that although the UFF parameterization reproduces the basic parameters of the crystal $LiBH_4$, the stong bond boron-hydrogen does not allow the break of the fragment BH_4. It is still possible to break these bonds at a longer time scale than that considered in this study (5 ns). We observe the formation of a peak in the hydrogen-hydrogen radial distribution function at 0.85 A, which indicates the formation of hydrogen molecule. By analyzing the trajectory of the atoms during the simulation, we can see that hydrogen molecules are mainly formed of hydrogen atoms originating from the structure of MgH_2. We could expect that the formed hydrogen molecules diffuse through the graphite structure and that it could be collected in a gas form.

However, the analysis of Fig. 3 shows that hydrogen is organized around graphite layers at an average distance of 2.5 A. In Fig. 4 we observe the formation of the pairs LiH with the interatomic distance of 2.0 A, a value close to the specific interatomic distance in the crystal LiH (about 2.042 A). The formation of hexagonal boron layers may force the Li-H couples to get organized in layers at the interface with the boron layers. The analysis of the mean square displacement of lithium and hydrogen atoms indicates a similar mobility for the two atomic species. Correlating this observation with the radial distribution function of the Li-H pairs one could imagine a diffusion mechanism of lithium and hydrogen atoms in pairs. The acummulation of such pairs in the depleted area in magnesium and boron atoms and the Li-H clusters may be the seed for the growth of the crystal LiH.

Taking into account the approximate empirical potential and the relatively small size of the interface model used in these studies, these results should be viewed critically, but they allow us to imagine the reaction mechanisms (1). For a high accuracy of the descriptions of the interactions between the atoms of Li, Mg, B, H and C in various environments we changed the Gulp program by introducing flexible and dissociative KKY potential,[21] which was proved to be very good for various minerals. This update of the code will allow us to describe more accurately the processes that take place at the two interfaces.

QM/MM Calculations for the interface $LiBH_4$ / MgH_2

After the equilibration of the system, the formation of four hydrogen molecules is observed at the interface. Analyzing the source of the atoms that form such hydrogen molecules we observe that they are originating from three fragments BH_4 and one fragment of MgH_2 located at the interface $LiBH_4$ / MgH_2. In addition, a molecule LiH is identified. Pairs of boron atoms with an average interatomic distance about 1.78 A (the distance specific to crystal MgB_2) are revealed.

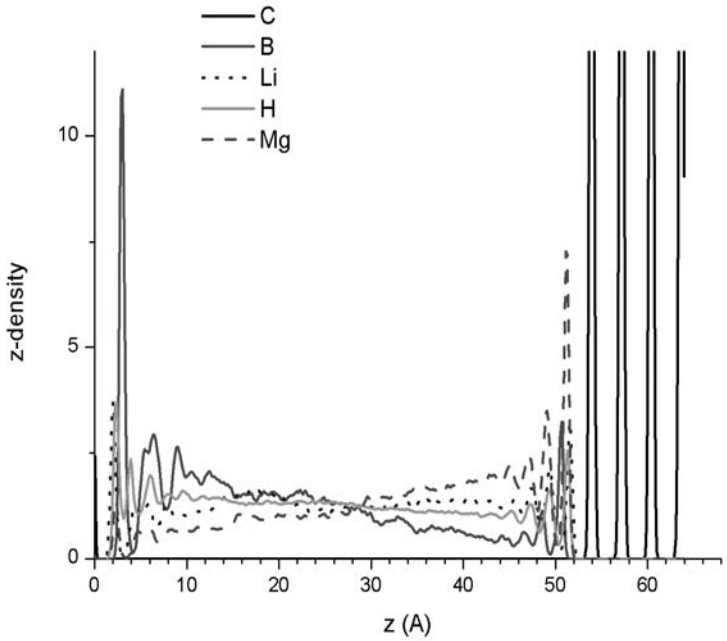

Fig. 3 – z-Density distribution of the atoms in the system.

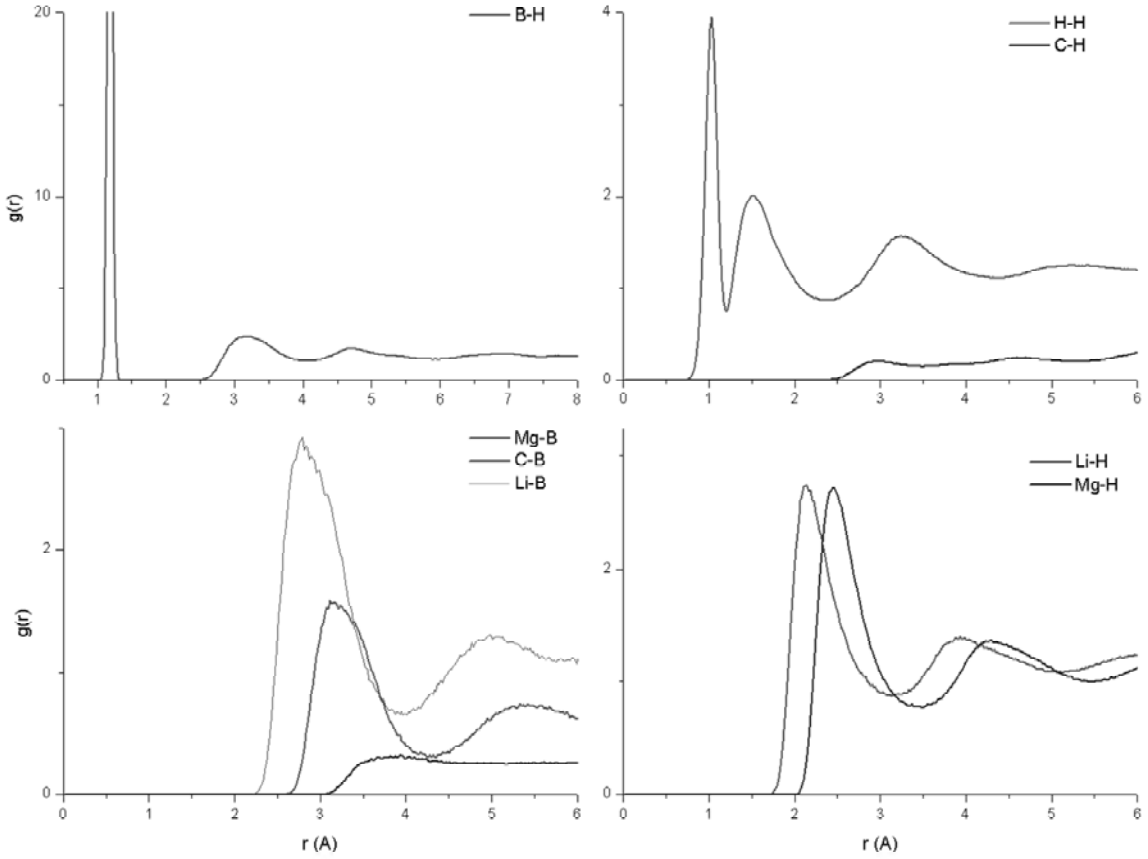

Fig. 4 – The radial distribution functions for different pairs of atoms in the system.

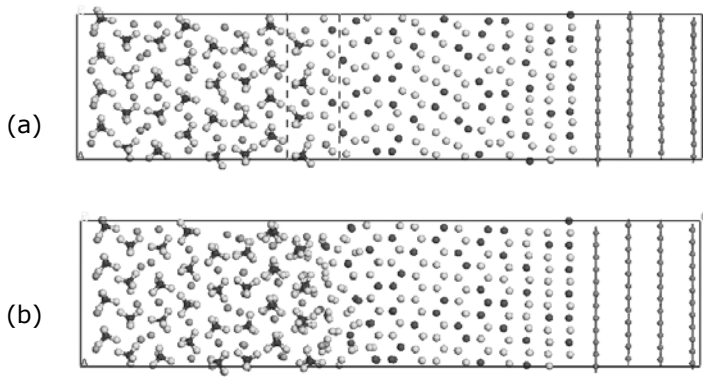

Fig. 5 – The initial (a) and optimized structure (b) within the ONIOM calculations.
The quantum area at the interface $LiBH_4/MgH_2$ is designed by dashed lines. The colour legend is the same as for Fig. 2.

CONCLUSIONS

In the present study the mechanisms of the reverse hydrogen storage at the interface $LiBH_4/MgH_2$/graphite are investigated in three stages. In the first stage, by doing some ab-initio thermodynamic calculations we established the thermodynamic conditions for which the reaction (1) is energetically efficient. Thus, we found that this reaction becomes exothermal above 280 K. Although the rate-limiting steps in a given storage reaction are not considered here, by doing similar thermodynamic calculations for the multistep reactions the favorable reaction paths can be established.

It is important to be aware that to know the favorable thermodynamics is a necessary, but not sufficient condition for the development of suitable hydrogen storage materials. To find the reaction mechanisms at the interface $LiBH_4/MgH_2$/ graphite

we continued our study with a second stage, at which we did some Molecular Dynamics simulations for such interfaces by using the empirical force field UFF. For better results we re-parameterized this force field, having as reference the equilibrium values determined within the DFT calculations of the lattice constants of the systems involved.

The atoms of the $LiBH_4$ and MgH_2 structures diffuse through the interface $LiBH_4$ / MgH_2 and are arranged in layers at the interface with the graphite layers. The graphite layers can act as a patern maker for the formation of a planar hexagonal network of boron like in MgB_2, one of the products of the reaction (1). Lithium and hydrogen atoms diffuse in pairs, being able to clusterize in the Mg and B depleted region. Such structures may act as seeds for the formation of the crystal LiH. The formed hydrogen molecules may diffuse through the system and graphite layers, beeing colected in gas phase.

To characterize the reaction (1) completly, we further investigated the interface $LiBH_4$ / MgH_2 at the third stage by some hybrid QM/MM calculations. The formation of new molecules or fragments of the reaction products during the geometry optimization of the interface $LiBH_4$ / MgH_2 indicates that the two crystaline systems are reactive. We have to emphasize that for such complex systems it is difficult to determine the reaction path or the rection energy from the QM/MM calculations alone.

Acknowledgements: The authors gratefully acknowledge the financial support provided by the National Authority for Scientific Research, Bucharest, Roumania through the project PNCDI-2No, 72196/2008 "New complex hydrides for hydrogen storage in hydrite tank suitable for vehicular applications" – STOHICO. The calculations were carried out by using the infrastructure developed under NASR Grant, Capacities Project CpI 84/2007.

REFERENCES

1. O. Friedrichs, A. Borgschulte, S. Kato, F. Buchter, R. Gremaud, A. Remhof, *Chem Eur J*, **2009**, *15*, 5531; A. Zuttel, S. Renth, P. Fischer, P.Wenger, P. Sudan, Ph. Mauron Ph, *J Alloys Compd*, **2003**, *515*, 356.
2. J.J. Vajo, S.L. Skeith, F. Mertens, *J Phys Chem B*, 2005, *109*, 3719; G. Barkhordarian,T. Klassen, M. Dornheim, R. Bormann, *J Alloys Compd,* **2007**, *440*, L18.
3. U. Bosenberg, S. Doppiu, L. Mosegaard, G. Barkhordarian, N. Eigen, A. Borgschulte, *Acta Mater,* **2007**, *55*, 3951; J.J. Vajo, T.T. Salguero, A.F. Gross, S.L. Skeith, G.L. Olson, *J Alloys Compd*, **2007**, *409*, 446; M.Q. Fan, L.X. Sun, Y. Zhang, F. Xu, J. Zhang, H.L. Chu, *Int. J. Hydrogen Energy*, **2008**, *33*, 74; G. Barkhordarian, T.R. Jensen, S. Doppiu, U. Bosenberg, A. Borgschulte, R. Gremaud, *J Phys Chem C*, **2008**, *112*, 2743.
4. C.Z. Wu, P. Wang, X. Yao, C. Liu, D.M. Chen, G.Q. Lu, H.M. Cheng, *J. Alloys and Compounds*, **2006**, *414*, 259.; P.-J. Wanga, Z.-Z. Fanga, L.-P. Maa, X.-D. Kanga si P. Wang, *Int. J. Hydrogen En.*, **2010**, *35*, 3072; Z.-Z. Fang, X.-D. Kang, P. Wang, *Int. J. Hydrogen En.*, **2010**, *35*, 8247.
5. S. Cahen, J.-B Eymery, R. Janot and J.-M. Tarascom, *J. Power Source*, **2009**, *189*, 902; P.-J. Wang, Z.-Z. Fang, L.-P. Ma, X.-D. Kang, P. Wang, *Int. J. Hydrogen En.*, **2008**, *33*, 5611; **2010**, *35*, 3072; X. Liu, D. Peaslee, C.Z. Jost and E.H. Majzoub, *J. Phys. Chem. C*, **2010**, *114*, 14036; A.F. Gross, J.J. Vajo, S.L. Van Atta, G.L. Oslo, S.L. Skeith si F. Mertens, *J. Phys. Chem. C,* **2008**, *112*, 5651; S. Cahen, J.B. Eymery, R. Janot si J.M. Tarascon, *J. Power Sources*, **2009**, *189*, 902; X. Liu, S. Peaslee, C.Z. Jost si E.H. Majzoub, *J. Phys. Chem. C*, **2010**, *114*, 14036.
6. G. J. Ackland, *J. Phys.: Condens. Matter*, **2002**, *14*, 2975.
7. K.J. Michael, A.R. Akbarzadeh and V. Ozolins, J.Phys.Chem. C, **2009**, *113*, 14551, A.R. Akbarzadeh, V. Ozolins and K.J. Michael, *Adv. Mater.*, **2007**, *19*, 3233.
8. G.-M. Rignanese, D. Sangalli, R. Shaltaf, M. Torrent, M.J. Verstraete, G. Zerah si J.W. Zwanziger, *Comp. Phys. Commun.,* **2009**, *180*, 2582; http://www.abinit.org
9. Y. Wang si J. P. Perdew, *Phys. Rev. B*, **1991**, *44*, 13298.
10. C. Wolverton, V. Ozolin and M. Asta, *Phys. Rev. B*, **2004**, *69*, 144109; G. Kresse, J. Furthmuller and J. Hafner, *Europhys. Lett.*, **1995**, *32*, 729; D. Alfe, G. D. Price, M. J. Gillan, *Phys. Rev. B,* **2001**, *64*, 045123.
11. S. Baroni, P. Gianozzi, and A. Testa, *Phys. Rev. Lett.*, **1987**, *58*, 1861.
12. "The General Utility Lattice Program", J.D. Gale and A.L. Rohl, *Mol. Simul.*, **2003**, *29*, 291; https://projects.ivec.org/gulp
13. A.K. Rappi, C.J. Casewit, K S. Colwell, W.A. Goddard III si W.M. Skid, *J. Am. Chem. Soc*., **1992**, *114*, 10025.
14. The force field parameters are available from the authors.
15. "Optimization of Parameters for Semiempirical Methods V: Modification of NDDO Approximations and Application to 70 Elements", J. J. P. Stewart, *J. Mol. Mod*., **2007**, *13*, 1173. http://www.springerlink.com/content/ar33482301010477/fulltext.pdf
16. http://openmopac.net/home.html
17. S. Dapprich, I. Komaromi, K.S. Byun, K. Morokuma and M.J. Frich, *J. Mol. Struct. (Theochem)*, **1999**, *462*,1.
18. http://www.gaussian.com/g_misc/g03/citation_g03.htm
19. A. Züttel, A. Borgschulte and S. Orimo, *Scripta Mater.*, **2007**, *56*, 823.
20. F. D. Murnaghan, *PNAS*, **1944**, *30*, 244.
21. Kumagai, N., K. Kawamura and T. Yokokawa. *Mol. Sim.*, **1994**, *12*, 177.